HIERARCHICAL SCALING LAWS FOR THE LONGITUDINAL STRENGTH AND TOUGHNESS OF COMPOSITES

S. Pimenta*, S.T. Pinho

Department of Aeronautics, Imperial College London, South Kensington Campus, SW7 2AZ London
**Corresponding author (soraia.pimenta07@imperial.ac.uk)*

Keywords: Hierarchical fibre bundles; Strength; Size effects; Statistics.

Abstract
This paper presents an analytical model for size effects on the longitudinal tensile strength of composite fibre bundles. Individual fibre strength is modelled by a Weibull distribution, while the matrix or interface is represented by a perfectly-plastic shear-lag model. A stochastic scaling law relating strength distributions of hierarchical bundles of different levels is derived, and an efficient numerical scheme (based on asymptotic limits) is proposed. Model predictions at different scales are validated against experimental results from the literature.

1 Introduction
Size effects on the strength of composite materials are widely reported in the literature and present a significant design challenge, but a universally accepted modelling strategy is still to be developed [1]. This paper presents a model for size effects on the longitudinal tensile strength of UniDirectional (UD) Fibre-Reinforced Polymers (FRPs), based on the stochastic variability of fibre strength and the definition of hierarchical fibre-matrix bundles [2].

Stochastic effects play a major role on the size vs. strength relation in FRP structures [1]. Under uniform (subscript U) stresses σ, the Weakest Link Theory (WLT) relates the survival probabilities of a reference element ($S_{\mathrm{U,r}}$) and of a chain of n elements ($S_{\mathrm{U,n}}$) by:

$$S_{\mathrm{U,n}}(\sigma) = \left[S_{\mathrm{U,r}}(\sigma)\right]^n \qquad \Rightarrow \qquad \ln\left[S_{\mathrm{U,n}}(\sigma)\right] = n \cdot \ln\left[S_{\mathrm{U,r}}(\sigma)\right] = \frac{l_{\mathrm{n}}}{l_{\mathrm{r}}} \cdot \ln\left[S_{\mathrm{U,r}}(\sigma)\right] \tag{1}$$

where l_{r} and l_{n} are the respective lengths of the reference element and the chain. Accordingly, Weibull [3] proposed a new type of distribution for the strength of brittle materials, so that the survival and failure probabilities of a chain under uniform stresses σ are:

$$S_{\mathrm{U,n}}(\sigma) = \exp\left[-\frac{l_{\mathrm{n}}}{l_{\mathrm{r}}}\left(\frac{\sigma}{\sigma_0}\right)^m\right] \qquad \text{and} \qquad F_{\mathrm{U,n}}(\sigma) = 1 - \exp\left[-\frac{l_{\mathrm{n}}}{l_{\mathrm{r}}}\left(\frac{\sigma}{\sigma_0}\right)^m\right] \tag{2}$$

where m and σ_0 are respectively the shape and scale (measured at l_{r}) parameters.

While Equations 1 and 2 have been widely used to model the length effect on the strength of technical fibres [4], their direct application to FRPs is inconsistent with the quasi-brittle failure exhibited by these materials [5-9]. It has been suggested [1] that fibre bundle models overcome this limitation and capture most of the physics involved in the longitudinal failure of FRPs.

Newman and Gabrielov's [10] *dry* fibre bundle model assumes a hierarchical failure process, which is supported by experimental observations of quasi-fractal fracture surfaces in FRPs [11-12]. Considering that a bundle of hierarchical level $[i+1]$ is composed by two sub-bundles of level $[i]$, they derived a recursive relation for bundle strength distributions:

$$F^{[i+1]}(\sigma) = F^{[i]}(\sigma) \cdot \left[2 \cdot F^{[i]}(2 \cdot \sigma) - F^{[i]}(\sigma)\right] \quad (3)$$

where $F^{[i]}(\sigma)$ is the failure probability of a level-$[i]$ bundle under an applied stress σ. This model does not consider the effect of an embedding matrix, and does not include a process zone length (which is paramount for quasi-brittle materials [9]).

This paper presents a new fibre-bundle model for predicting size effects on the longitudinal tensile strength of FRP (embedded) bundles [2]. Following Newman and Gabrielov's work [10], bundles are hierarchically organised and scaling is based on the single-fibre strength distribution. However, the matrix (or fibre-matrix interface) is now considered through a simplified shear-lag model, with substantial implications on the derivation of the scaling law.

In this paper, Section 2 presents the formulation of the model, subsequently validated against experimental data in Section 3; Section 4 discusses results and draws the main conclusions.

2 Model development

2.1 Methodology and definitions

This model is based on hierarchical fibre-matrix bundles (Figure 1a). Section 2.2 defines their geometry and the respective shear-lag boundary (Γ_{SL}), which includes the effect of the matrix or fibre-matrix interface. This results in non-uniform stress fields near fibre breaks, hence the corresponding failure probabilities are derived in Section 2.3.

Section 2.4 derives the hierarchical law for bundle failure, firstly considering the failure process of a 2-fibres bundle; the resulting relation between fibre and bundle strength distributions is then used recursively throughout bundle hierarchy. The numerical implementation of the model and derivation of asymptotic limits are described in Section 2.5.

This paper expresses longitudinal stresses (σ) as fibre stresses. The concept of stochastic strength is extended to non-uniform stress fields, characterised by a shape function Φ and remote stress σ^{∞}. Under such field, the strength of an element $\mathcal{E}$ with length ℓ is represented as $X^{\mathcal{E}}_{\Phi,\ell}$; the associated *failure probability* is $F^{\mathcal{E}}_{\Phi,\ell}(\sigma^{\infty}) = \Pr(X^{\mathcal{E}}_{\Phi,\ell} \leq \sigma^{\infty})$, and the corresponding *survival probability* is $S^{\mathcal{E}}_{\Phi,\ell}(\sigma^{\infty}) = 1 - F^{\mathcal{E}}_{\Phi,\ell}(\sigma^{\infty})$.

2.2 Fibre bundle geometry and shear-lag boundary

Figure 1a shows a set of hierarchical fibre bundles; these are formed by pairing individual fibres (level-[0]) into a level-[1] bundle, and then sequentially grouping two level-$[i]$ bundles into one level-$[i+1]$ bundle. The number of fibres in a level-$[i]$ bundle is thus $n^{\mathrm{f}} = 2^i$.

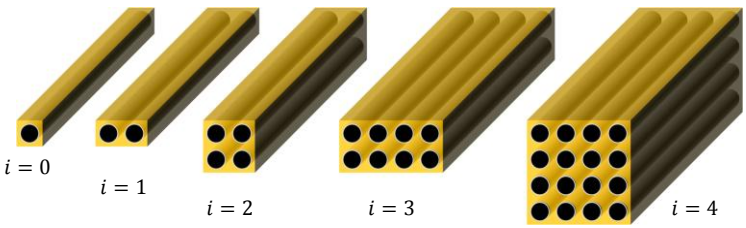

a) Bundle hierarchy.

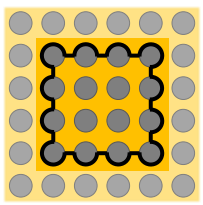

b) Shear-lag boundary.

Figure 1. Hierarchical bundles and shear-lag boundary.

The fibres (superscript f) are arranged in a quadrangular architecture, characterised by the fibre diameter ϕ^{f} (associated circumference C^{f} and area A^{f}) and volume fraction V^{f}.

Consider now a level-$[i]$ bundle with a broken section, embedded in a larger composite bundle. One can define a level-$[i]$ *shear-lag boundary* as the surface at which shear-lag stresses will be transferred between the unbroken surrounding material and the broken level-$[i]$ bundle. Several configurations can be defined [2]; assuming preferential splitting along the fibre-matrix interface (Figure 2b), the perimeter of the shear-lag boundary is:

$$C^{[i]} = 3 \cdot C^{\mathrm{f}} + 4 \cdot \left[\left(\sqrt{n^{\mathrm{f}}} - 1 \right) \cdot s + \left(\sqrt{n^{\mathrm{f}}} - 2 \right) \cdot \frac{C^{\mathrm{f}}}{2} \right] \qquad \text{with} \qquad s = \left(\frac{\sqrt{\pi}}{2\sqrt{V^{\mathrm{f}}}} - 1 \right) \cdot \phi^{\mathrm{f}} \tag{4}$$

2.3 Survival probabilities under several loading conditions

The WLT (Equation 1) can be generalised to non-uniform chain stresses. Consider a chain of length l under a linear tensile stress field (subscript L, Figure 2b):

$$\sigma_{\mathrm{L}}(x) = \frac{\sigma^{\infty}}{l} \cdot x \quad , \qquad x \in [0, l] \tag{5}$$

Dividing the linearly-loaded chain into $n \to \infty$ links of individual length $\Delta x = l/n$, its survival probability S_{L} under $\sigma_{\mathrm{L}}(x)$ relates to that of a uniformly loaded chain (S_{U}) by:

$$\ln[S_{\mathrm{L}}(\sigma^{\infty})] = \lim_{n\to\infty} \sum_{j=1}^{n} \frac{\Delta x}{l} \cdot \ln\left[S_{\mathrm{L}}\left(\sigma_{\mathrm{L}}(x_j) \right) \right] = \frac{1}{\sigma^{\infty}} \int_{\sigma_{\mathrm{L}}=0}^{\sigma^{\infty}} \ln[S_{\mathrm{U}}(\sigma^{\infty})] \, \mathrm{d}\sigma_{\mathrm{L}} \tag{6}$$

For the particular case of a material with Weibull strength distribution,

$$S_{\mathrm{L}}(\sigma^{\infty}) = \exp\left[-\frac{1}{1+m} \cdot \left(\frac{\sigma}{\sigma_0} \right)^{m} \right] \tag{7}$$

Consider now a chain of length l under a linear stress concentrations field with factor k (subscript K, Figure 2c):

$$\sigma_{\mathrm{K}}(x) = \sigma^{\infty} + \frac{\sigma^{\infty} \cdot (k-1)}{l} \cdot x \quad , \qquad x \in [0, l] \tag{8}$$

Using the same procedure as for the pure linear stress case, the survival probability S_{K} under $\sigma_{\mathrm{K}}(x)$ relates to that of a uniformly loaded chain (S_{U}) and of a linearly loaded chain (S_{L}) by:

$$\ln[S_{\mathrm{K}}(\sigma^{\infty})] = \begin{cases} \dfrac{1}{\sigma^{\infty}(k-1)} \displaystyle\int_{\sigma_{\mathrm{K}}=\sigma^{\infty}}^{k\cdot\sigma^{\infty}} \ln[S_{\mathrm{U}}(\sigma_{\mathrm{K}})] \, \mathrm{d}\sigma_{\mathrm{K}} = \dfrac{k \cdot \ln[S_{\mathrm{L}}(k \cdot \sigma^{\infty})] - \ln[S_{\mathrm{L}}(\sigma^{\infty})]}{k-1} & , k \neq 1 \\ \ln[S_{\mathrm{U}}(\sigma^{\infty})] & , k = 1 \end{cases} \tag{9}$$

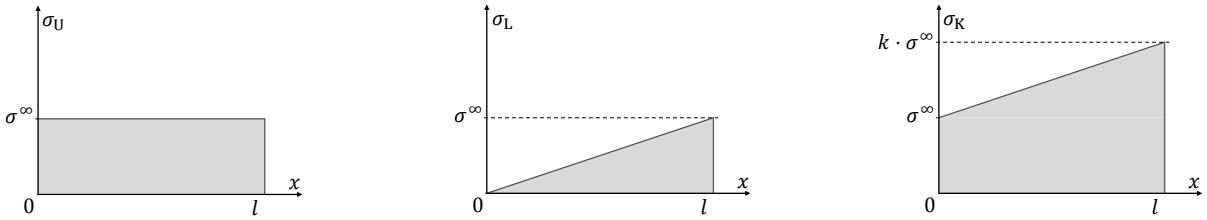

a) Uniform loading. b) Pure linear loading. c) Linear stress concentrations.

Figure 2. Stress fields analysed through a generalised weakest link theory.

For the particular case of a material with Weibull strength distribution,

$$S_{\mathrm{K}}(\sigma^{\infty}) = \exp\left[-\mathcal{C}_{\mathrm{K}} \cdot \left(\frac{\sigma}{\sigma_0}\right)^{m}\right] \qquad \text{with} \qquad \mathcal{C}_{\mathrm{K}} = \frac{k^{m+1}-1}{(m+1)\cdot(k-1)} \tag{10}$$

2.4 Hierarchical law for bundle failure

Consider a level-[1] bundle of length l_{r} (composed by two embedded level-[0] fibres) under the remote stress σ^{∞}, and assume that fibre $\mathcal{A}$ is failed at $x = 0$ (Figure). Following a perfectly-plastic shear-lag model (with strength T_{SL} and shear-lag perimeter from Equation 4), the level-[0] *effective recovery length* (subscript e) – within which fibre $\mathcal{A}$ linearly recovers the remote stresses, and fibre $\mathcal{B}$ undergoes linear stress concentrations (with $k = 2$) – is:

$$l_{\mathrm{e}}^{[0]}(\sigma^{\infty}) = 2 \cdot \frac{n^{\mathrm{f}} \cdot A^{\mathrm{f}}}{C^{[0]} \cdot T_{\mathrm{SL}}} \cdot \sigma^{\infty} \qquad \text{with} \qquad n^{\mathrm{f}} = 1 \quad \text{for} \quad i = 0 \tag{11}$$

Bundle failure requires that both fibres $\mathcal{A}$ and $\mathcal{B}$ break in nearby locations, so that the shear-lag boundary yields completely between breaks (Figure 4b). Therefore, once fibre $\mathcal{A}$ fails, the level-[1] control length – within which a break in fibre $\mathcal{B}$ leads to bundle failure – is:

$$l_{\mathrm{c}}^{[1]}(\sigma^{\infty}) = 2 \cdot l_{\mathrm{e}}^{[0]}(\sigma^{\infty}) \tag{12}$$

The control region is partitioned into 4 fibre segments ($\mathcal{A}_1$, $\mathcal{A}_2$, $\mathcal{B}_1$ and $\mathcal{B}_2$) of equal length $l_{\mathrm{e}}^{[0]}$ (Figure 4c). It is assumed that fibre strength under uniform stresses follows a Weibull distribution with parameters m and σ_0^{f} at l_{r}, and survival probability $S_{\mathrm{U,r}}^{[0]}$. This is used to calculate fibre-segment survival probabilities under uniform stresses (yielding $S_{\mathrm{U,e}}^{[0]}$ through Equation 1) and linear stress concentration (yielding $S_{\mathrm{K,r}}^{[0]}$ through Equation 9, and $S_{\mathrm{K,e}}^{[0]}$ through Equation 1) .

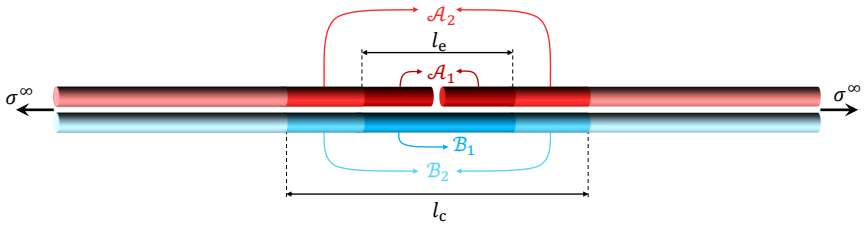

a) Failure of fibre $\mathcal{A}$: definition of fibre segments and the effective recovery (l_{e}) and control (l_{c}) lengths.

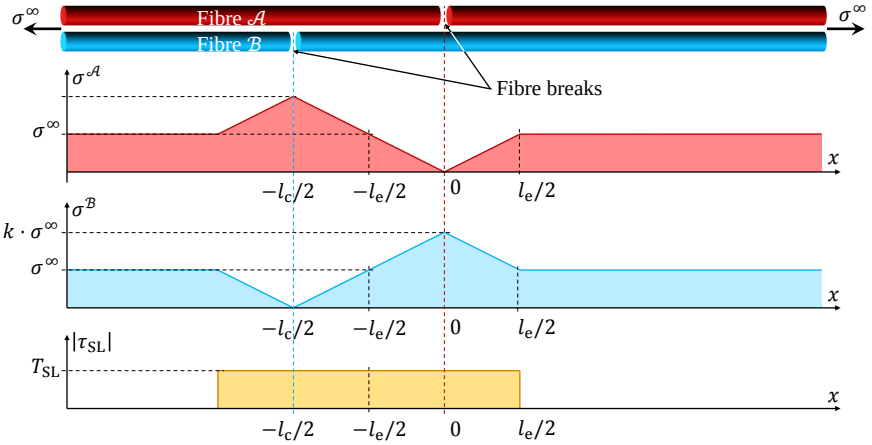

b) Stress fields during bundle failure and definition of critical distance between fibre breaks: the bundle fails only if fibre $\mathcal{B}$ breaks at a distance smaller than $l_{\mathrm{c}}/2$ from the break in fibre $\mathcal{A}$.

Figure 3. Stress fields and length scales in a level-[1] fibre bundle.

Considering that
(i) the bundle (length l_r) is represented by a chain of independent control regions of length l_c;
(ii) within each control region, each fibre can break only once;
the bundle survival probability can be calculated as [2]:

$$S_{U,c}^{[1]}(\sigma^{\infty}) = \left(S_{U,e}^{[0]}(\sigma^{\infty})\right)^4 + 2 \cdot \left[1 - \left(S_{U,e}^{[0]}(\sigma^{\infty})\right)^2\right] \cdot S_{U,e}^{[0]}(\sigma^{\infty}) \cdot S_{K,e}^{[0]}(\sigma^{\infty}) \quad (13)$$

Physically, Equation 13 states that *the bundle survives either if all its 4 segments survive, or if the weakest fibre fails and the strongest one survives the resulting stress field*. Assuming a self-similar hierarchical failure process, Equation 13 can be extrapolated to any bundle level, thus relating the survival probability of a level-$[i]$ bundle within its effective recovery length (defined as in Equation 11, with $[0] \rightarrow [i]$) to that of a $[i+1]$ bundle within its control length (defined as in Equation 12, with $[1] \rightarrow [i+1]$).

2.5 Asymptotic limits and numerical implementation

For $i > 0$, bundle strength distribution are non-Weibull, so $S_{K,r}^{[i]}(\sigma^{\infty})$ must be computed using Equation 9. This requires calculating $S_{U,r}^{[i-1]}(k \cdot \sigma^{\infty})$ and, consequently, $S_{U,r}^{[0]}(k^i \cdot \sigma^{\infty})$, which becomes intractable as bundle level increases. Opportunely, it can be demonstrated [2] that, if $\mathcal{C}_K > 3$ (valid for most technical fibres), Equation 13 (defined at any bundle level) tends asymptotically to the WLT for large stresses, and therefore:

$$S_{U,r}^{[i]}(\sigma^{\infty}) \xrightarrow{\sigma^{\infty} \rightarrow +\infty} \exp\left[-\left(\frac{\sigma^{\infty}}{2^{-\frac{i+1}{m}} \cdot \sigma_0}\right)^m\right] \Rightarrow \ln\left[S_{K,r}^{[i]}(\sigma^{\infty})\right] \xrightarrow{\sigma^{\infty} \rightarrow +\infty} \mathcal{C}_K \cdot \ln\left[S_{U,r}^{[i]}(\sigma^{\infty})\right], \quad \text{if } \mathcal{C}_K > 3 \quad (14)$$

An overview of the numerical implementation of the present model, which makes use of the asymptotes identified in Equation 14, is shown in Figure 4 [2]. Using array programming (e.g. MATLAB) greatly simplifies the implementation and reduces running time.

3 Model results and validation

Figures 5 and 6 compare the results obtained by the analytical model to experimental data from the literature [6-8]. The materials considered are described in Tables 1 and 2; raw fibre and matrix properties were used as model inputs, unless stated otherwise.

Figure 5 shows the calculated strength probability map for bundles of the same material (referenced as T^nT [6]) but different filament counts; the full set of converged strength distributions was obtained in less than 1 second with an Intel® Core™ 2 Quad CPU @ 2.50 GHz. The model predicts an initial strengthening throughout bundle hierarchy, after which strength decreases; scatter is monotonically reduced with increasing bundle sizes.

Figure 6 presents strength distributions of several micro-composites (referenced as A^4S, A^4F, I^7S and I^7F [7-8]) combining distinct carbon fibres, epoxy matrices and geometries. The model reproduces the different slopes and locations of the four experimental data sets, as well as the curvature of micro-bundle strength distributions plotted in Weibull coordinates.

Comparing the predictions from the present model against those of Newman and Gabrielov (Equation 3 [10]), it is shown that considering the presence of the matrix in the former substantially increases the mean value and reduces the variability of bundle strengths. The effect of the matrix is more pronounced as it shear strength increases (see Figure 6, where resin type S is significantly stronger than resin type F).

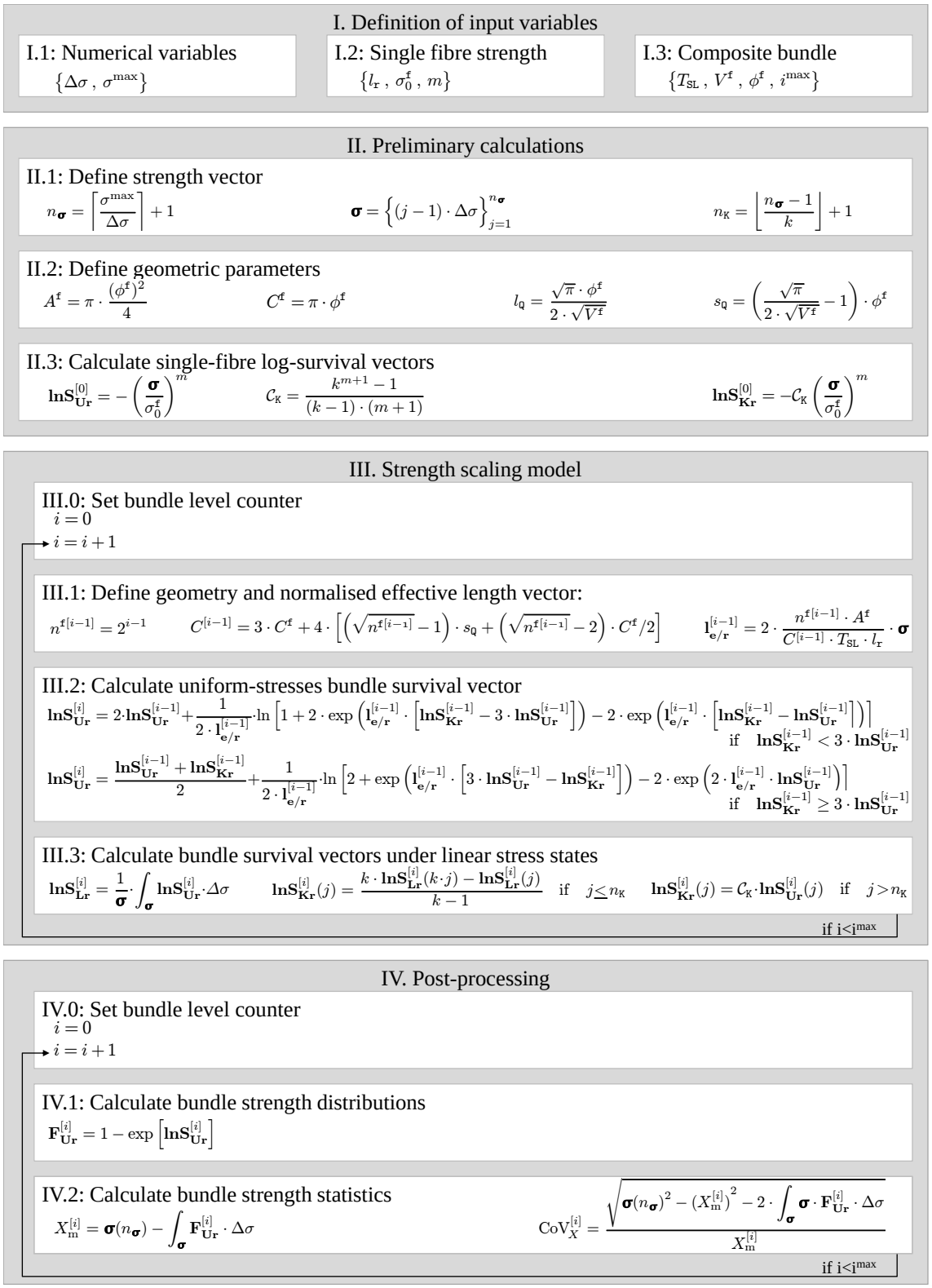

Figure 4. Numerical implementation of the bundle strength model.

4 Discussion and conclusions

An analytical model for size effects on the longitudinal tensile strength of FRP bundles was developed, implemented and validated. The model is based on the stochastic analysis of the failure process in hierarchical bundles, considering Weibull fibres and a simplified shear-lag model to represent matrix effects.

Composite reference	Fibre reference	n^{f}	Matrix reference	T_{SL} (MPa)	V^{f} (%)	Reference
$\mathrm{T^nT}$	T	$10^4 - 10^6$	T	52.4	60	[6]
$\mathrm{A^4S}$	A	4	S	46.6	70	[7]
$\mathrm{A^4F}$	A	4	F	10.3	70	[7]
$\mathrm{I^7S}$	I	7	S	46.6	56	[8]
$\mathrm{I^7F}$	I	7	F	10.3	56	[8]

Table 1. Description of composites used for model validation.

Fibre reference	Fibre type	ϕ^{f} (μm)	$l_{\mathrm{r}}^{\mathrm{f}}$ (mm)	m	σ_0^{f} (GPa)	Reference
T	T800	5.00	50	3.8	3.570	[6]
A	AS4	6.85	10	4.8	4.493	[7]
I	IM6	5.63	10	5.4	5.283	[8]

Table 2. Carbon-fibre data for model validation.

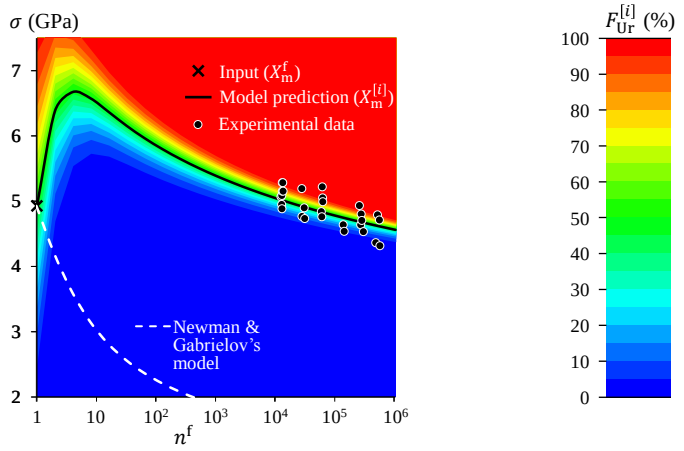

Figure 5. Size effect on bundle strength ($\mathrm{T^nT}$ material): experimental bundle strengths (data points [6]), present model's probability map (with mean strength highlighted), and Newman and Gabrielov's [10] mean strength prediction (dashed line in Figure a). Model predictions assume $T_{\mathrm{SL}} = 79.6$ MPa. Both measurements and predictions were obtained for 10 mm long bundles.

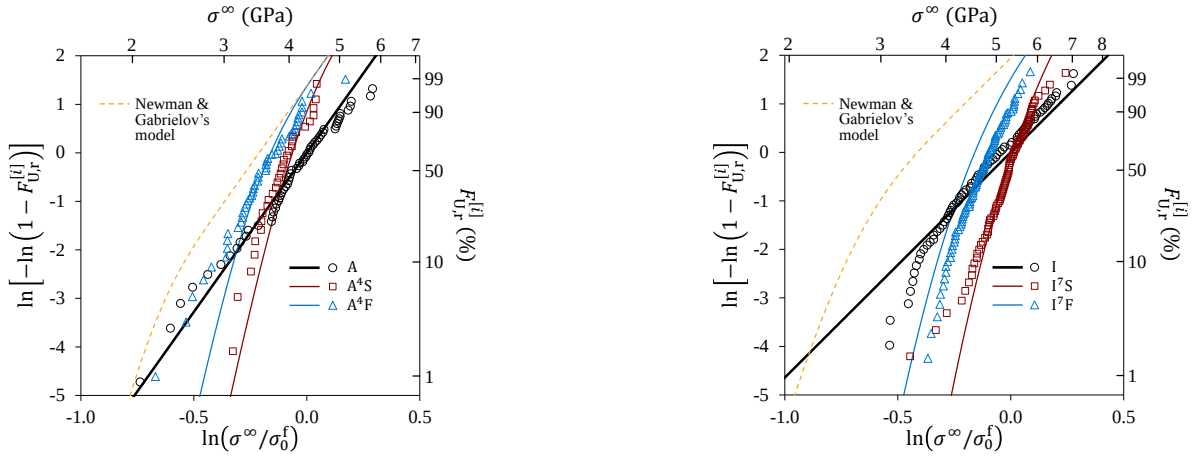

a) AS4 fibre type (considering $m = 6.6$, $\sigma_0^{\mathrm{f}} = 4.3$ GPa at $l_{\mathrm{r}} = 10$ mm.).

b) IM7 fibre type (considering $m = 4.6$, $\sigma_0^{\mathrm{f}} = 5.3$ GPa at $l_{\mathrm{r}} = 10$ mm.).

Figure 6. Strength distributions (Weibull plots) for micro-composites: experimental results (data points [7-8]), visually fitted single-fibre distribution for model input (thick lines), present model predictions for both resin types (thin lines), and Newman and Gabrielov's model [10] predition (dashed lines). Model results take into account free-edge effects [2].

The model predicts full strength distributions and statistics for bundles of any size. The matrix (or interface) was shown to have a significant strengthening effect, which supports the present model over others not including this feature (e.g. WLT and Newman and Gabrielov's [10]). The numerical implementation scheme based based on asymptotic limits resulted into extremely short running times (less than 1 second), thus enabling its application for detailed parametric studies [2] and Monte-Carlo analyses.

The model was validated at the micro and macro scales, showing a remarkable agreement with measured bundle strengths in a large range of scales. A more detailed analysis [2] reveals that other experimentally observed features – e.g. the quasi-brittle nature of composites and the fair agreement of large-scale size effects with the WLT – are captured as well.

Predictive models for size effects in composite materials are paramount for scaling small-coupon experimental results to the design of large structures. Moreover, the present work provides insight on the longitudinal tensile failure process [2]. The model's ability to compute strength distributions for small bundles (rather than only for asymptotically large ones) makes it particularly suitable for state-of-the-art multiscale discontinuous composites [12-13]. Further developments and applications include predicting the shape of fracture surfaces and the corresponding fracture toughness for FRPs under longitudinal tensile failure.

References

[1] Wisnom M.R. Size effects in the testing of fibre-composite materials. *Compos Sci Technol*, **59**, pp. 1937-1957 (1999).
[2] Pimenta S., Pinho S.T. Hierarchical scaling law for the strength of composite fibre bundles. *J Mech Phys Solids* (submitted, 2012).
[3] Weibull G.W. A statistical distribution function of wide applicability. *J Appl Math*, pp. 293-297 (1951).
[4] Pradhan S. et al. Failure processes in elastic fiber bundles. *Rev Mod Phys*, **82**, pp. 499-555 (2010).
[5] Scott A.E. et al. In situ fibre fracture measurements in carbon-epoxy laminates using high-resolution computed tomography. *Compos Sci Technol*, **71**, pp. 1471-1477 (2011).
[6] Okabe T., Takeda N. Size effect on tensile strength of unidirectional CFRP composites – experiment and simulation. *Compos Sci Technol*, **62**, pp. 2053-2064 (2002).
[7] Beyerlein I.J., Phoenix .I.J. Statistics for the strength and size effects of microcomposites with four carbon fibers in epoxy resin. *Compos Sci Technol*, **56**, pp. 75-92 (1996).
[8] Kazanci M. Carbon fiber reinforced composites in two different epoxies. *Polym Test*, **23**, pp. 747-753 (2004).
[9] Bazant Z.P. Size effect on structural strength: a review. *Arch Appl Mech*, **69**, pp. 703-725 (1999).
[10] Newman W.I., Gabrielov A.M. Failure of hierarchical distributions of fiber-bundles. 1. *Int J Fracture*, **50**, pp. 1-14 (1991).
[11] Laffan M.J. et al. Measurement of the in situ ply fracture toughness associated with mode I fibre tensile failure in FRP. Part II: Size and lay-up effects. *Compos Sci Technol*, **70**, pp. 614-621 (2010).
[12] Pimenta S. et al. Mechanical analysis and toughening mechanisms of a multiphase recycled CFRP. *Comp Sci Technol*, **70**, pp. 1713-1725 (2010).
[13] Harper L.T. et al. Characterisation of random carbon fibre composites from a directed fibre preforming process: The effect of tow filamentisation. *Comp Part A*, **38**, pp. 755-700 (2007).